A comparison of emissive probe techniques for electric potential measurements in a complex plasma

J. P. Sheehan,[1,a)] Y. Raitses,[2] N. Hershkowitz,[1] I. Kaganovich,[2] and N. J. Fisch[2]
[1]*Department of Engineering Physics, University of Wisconsin, Madison, Madison, Wisconsin 53706, USA*
[2]*Princeton Plasma Physics Laboratory, P.O. Box 451, Princeton, New Jersey 08543-0451, USA*

(Received 9 March 2011; accepted 31 May 2011; published online 1 July 2011)

The major emissive probe techniques are compared to better understand the floating potential of an electron emitting surface in a plasma. An overview of the separation point technique, floating point technique, and inflection point in the limit of zero emission technique is given, addressing how each method works as well as the theoretical basis and limitations of each. It is shown that while the floating point method is the most popular, it is expected to yield a value $\sim 1.5T_e/e$ below the plasma potential due to a virtual cathode forming around the probe. The theoretical predictions were checked with experiments performed in a 2 kW annular Hall thruster plasma ($n_e \sim 10^9-10^{10}$ $cm^{-3}$and $T_e \sim 10-50$ eV). The authors find that the floating point method gives a value around $2T_e/e$ below the inflection point method, which is shown to be a more accurate emissive probe technique than other techniques used in this work for measurements of the plasma potential.
 [doi:10.1063/1.3601354]

I. INTRODUCTION

Emissive probes have been effective in measuring the plasma potential in a wide variety of plasmas from RF discharges to tokamaks.[1,2] But it will be shown that the three most popular techniques—the separation point method,[3,4] the floating point method,[5] and the inflection point in the limit of zero emission method[6]—do not always give the same measure of the plasma potential. The experiment reported in this article seeks to resolve this discrepancy and determine which method, if any, measures the plasma potential most accurately.

A related question is that of the floating potential of an emitting surface. Theory states that the floating potential of a highly emitting surface will be T_e/e below the potential at the sheath edge,[7] but Particle in Cell (PIC)[2] simulations show that the potential drop depends on the ion temperature and may be $1.5T_e/e$ with cold ions, where T_e is electron temperature in eV.[8] Before now there have been no experiments to determine the real value of that potential drop across the sheath near a floating, emitting boundary.

II. POTENTIAL PROFILE NEAR AN EMITTING SURFACE

Intimately associated with the question of emissive probe operation is that of the potential profile near an emitting surface. Specifically of interest is a floating emissive surface, which was first considered by Hobbs and Wesson for an isotropic Maxwellian plasma with a planar geometry, ignoring the presheath.[7] For a non-emitting floating surface, there are two fluxes, collected electrons and collected ions, which cause a sheath to form at the surface with a potential drop from the sheath edge to the emitting surface of $\Delta V = -(T_e/e)\ln\left(\sqrt{m_i/(2\pi m_e)}\right)$, where ΔV is the potential drop from the sheath edge to the surface, m_e is the electron mass, and m_i is the ion mass. By including emission, which adds an additional flux of electrons from the probe, the magnitude of the potential drop from the bulk plasma to the surface decreases, which increases the floating potential. The potential drop can be written as

$$\Delta V = -(T_e/e)\ln\left(\frac{1-\Gamma}{\sqrt{2\pi m_e/m_i}}\right), \tag{1}$$

where Γ is the ratio of emitted electron flux to collected electron flux. Once Γ reaches the critical value of $\Gamma_c = 1 - 8.3\sqrt{m_e/m_i}$, the floating potential saturates at

$$\Delta V \approx -T_e/e. \tag{2}$$

These calculations done by Hobbs and Wesson describe the potential drop across the sheath, ignoring the presheath. Subsequent analyses have shown that the potential drop is $\approx -0.95T_e/e$.[9] At critical emission the presheath drop is approximately $0.8T_e/e$,[10] so, ultimately, the potential difference between the floating surface and the bulk plasma $(V_F - V_P)$ is

$$V_F - V_P \approx -1.8T_e/e. \tag{3}$$

Again, this result is for planar geometry. Above the critical emission level, a virtual cathode forms around the emitting surface.[11] The virtual cathode is caused by space charge that builds up around the probe at high emission levels due to the large electron flux from the probe. If the emission current is further increased beyond the saturation point, the floating potential will further increase, but will rise proportionally to the temperature of the probe wire (T_w) rather than the plasma electron temperature,[12] which is qualitatively consistent with early floating emissive probe data.[5]

[a)]Electronic mail: sheehan2@wisc.edu. URL: http://www.cae.wisc.edu/~sheehan.

Schwager investigated the potential drop across a planar sheath using PIC codes to simulate a deuterium plasma.[8] The end walls had secondary electron coefficients on the order of 1, so there was significant emission from the walls and although the plasma source was Maxwellian, the bulk plasma was not necessarily so. For cold ions ($T_i/T_e = 0.1$, which is assumed to be the case for Hall thrusters, which are considered in this paper[13]) and the secondary emission coefficient above the critical value, the potential drop through the sheath was $0.75T_e/e$ and the potential drop from the bulk to the wall was $1.5T_e/e$. This result is comparable to the analytic solution given by Hobbs and Wesson.

The floating potential of a cylindrical emitter does not have the rigorous analytical theory that the planar geometry does nor does it receive the same attention in simulations. Geometry does not affect the floating potential of Langmuir probes,[14] but geometry may affect how the sheath changes when emission is included. It is known that the presheath potential drop near a cylindrical surface is larger than that near a planar surface due to geometry effects and it depends on the radius of the probe.[15] These factors may affect the resulting floating potential of a highly emitting cylindrical probe differently than a planar wall.

III. OVERVIEW OF TECHNIQUES THAT WERE COMPARED

A. Separation point technique

The separation point technique is based on the assumption that an emissive probe will emit electrons below the plasma potential but not above it, which assumes that the electrons are emitting with zero energy and space charge effects are negligible.[16] A measure of the plasma potential can be made by taking two current-voltage (I-V) characteristic traces of the probe—one when cold and one when heated to emission—and determining the point at which the two traces diverge.[3,4] The probe bias at which the two traces diverge would be a measure of the plasma potential. However, since the emitting probe is putting extra electrons into the plasma, space charge effects may be significant, especially near the probe. This factor casts doubt on the validity of the separation point technique.

Secondary electron emission (SEE) may in principle have a significant effect on the current of I-V traces since the SEE coefficient (γ) can be as high as 0.5 for tungsten in a $T_e = 30$ eV plasma.[17] The majority of secondary electrons are emitted with energies of a few eV. When the probe is biased below the plasma potential, all SEE electrons are emitted into the plasma, meaning that for a cold probe, the electron current measured by the probe is less than the plasma electron current by a factor of $(1-\gamma)$. When the probe is biased above the plasma potential, the SEE electrons are confined by the potential barrier, so the SEE current in that region is expect to decrease exponentially with increasing bias. The effects for biases above the plasma potential may result in a rounded knee. Cold probes can suffer from surface contamination, which changes the work function of the surface, while emissive probes do not and γ depends on the work function, so SEE may adversely affect the separation point technique.

B. Floating point technique

Due to its ease of use, the most popular emissive probe method for measuring the plasma potential is, by far, the floating point method first presented by Kemp and Sellen.[5] The theory behind this method is intimately linked to that described in Sec. II. As the emission level increases, V_F rises and then saturates. The plasma potential is taken to be the potential of the probe at saturation. This makes the floating point method extremely convenient because it is a quick, simple measurement to take. Additionally, it can be used to easily measure the plasma potential as it evolves temporally[18] or, if the probe is moved, spatially.[19] The greatest source of error, however, comes from the fact that the floating potential saturates on the order of T_e/e below the plasma potential when space charge effects are considered.[7] If the temperature is small and constant, this effect will merely give the plasma potential measurements a small and constant offset.[20] If the temperature is large ($eV_p/T_e \lesssim 1$), however, this offset can be significant and if temperature gradients are present, the electric field derived from potential measurements will be incorrect. This technique has been often used in Hall thruster experiments described in previous papers;[12,13,21] one of these experiments has considered space charge effects according to Schwager's predictions and orbital motion limit effects.[13] Additionally, the floating point technique is the most commonly used emissive probe technique for fusion plasmas.[22,23]

C. Inflection point in the limit of zero emission technique

The inflection point in the limit of zero emission technique was developed to minimize the space charge effects that plague the floating point method.[6] The inflection point of an I-V trace would occur at the plasma potential, but space charge effects shift it to a more negative potential when measurements are taken in the bulk.[24] By taking multiple I-V traces at low levels of emission (emission currents on the order of the electron saturation current or less) and linearly extrapolating the inflection point to zero emission, space charge effects on the measurement are greatly reduced. Linear extrapolation accounts for space charge effects to the first order. Secondary electrons are not expected to affect the validity of this technique. If there is SEE current, it effectively reduces the electron saturation current. Because the inflection point in the limit of zero emission does not depend on the electron saturation current, SEE should have no effect on the technique.

The original paper presenting the inflection point method contained no theoretical basis for the linear extrapolation, only that the data looked approximately linear. A better understanding can be gained by using Ye and Takamura's analytical description of an emissive probe.[25] They derived a set of analytical equations which can be used to generate a theoretical emissive probe I-V trace by assuming that ions are cold, plasma electrons are Maxwellian, emitted electrons are

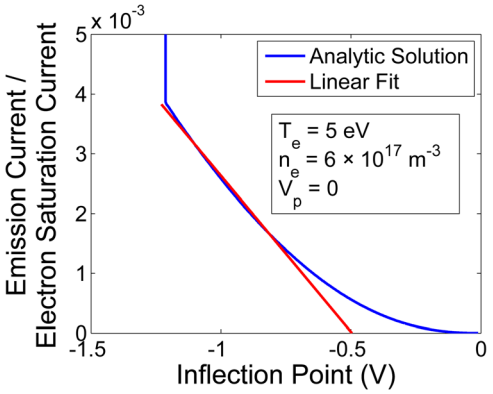

FIG. 1. (Color online) A graph of the theoretical relationship between emission current and the inflection point. A line is fit to the roughly linear region, as would be done when performing the inflection point in the limit of zero emission technique and extrapolated to 0.5 V. The plasma potential is set to 0 V.

emitted with negligible energy, the collector geometry is cylindrical, and the emitter geometry is planar. The greatest weakness of this model is the planar emitter. In reality, emissive probes are almost always cylindrical, but solving Poisson's equation with emission in this geometry has never been done. The error resulting from this approximation is discussed at the end of this section.

A large number of *I-V* traces, and, subsequently, inflection points, can be calculated with this model. For a range of probe temperatures, the *I-V* traces were calculated and the temperature limited emission and inflection point were determined. These two values correspond to a single data point on the inflection point versus normalized emission current graph in Fig. 1. Notice that the vertical axis shows emission current normalized to electron saturation current. Three general regions of this graph can be identified. First, at lowest emissions, the graph is nonlinear, but as the current increases it straightens into a region that is roughly linear. When the emission is high enough, the inflection point becomes independent of the emission current. All of these features can be identified in real data such as those shown in Fig. 2.

The major difference between the theory and experiment is the difference in scale of the vertical axes in Figs. 1 and 2. The data show emission levels that are three orders of magnitude above the theoretical levels. This difference is due to the fact that the theory is based on a planar emitter. In the first paper, on the inflection point in the limit of zero emission technique, it was noted that the emission scale decreased by a factor of ten when the probe wire radius was increased from 0.003 cm to 0.03 cm, while both gave the same measure of the plasma potential.[6] This trend suggests that the more planar a probe is (i.e., the larger the radius) the smaller the emission scale is on the emission versus inflection point graph. Extrapolating, one would expect that a planar emitter would have a much smaller emission range corresponding to the linear region than a cylindrical emitter. This could be due to the difference in space charge around probes of different radii, which occurs because the ion density profile in the sheath is steeper in cylindrical geometry. The authors conclude that Takamura's theoretical description of emissive probes still gives good qualitative support that the inflection point in the limit of zero emission method is accurate to within $(T_e/e)/10$.

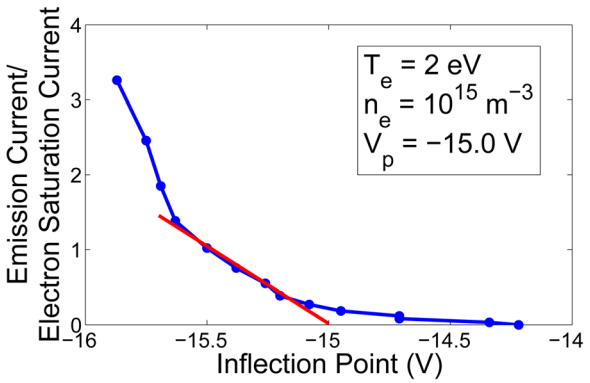

FIG. 2. (Color online) Real data showing the relationship between emission current and the inflection point. The plasma potential cited is that measured by the inflection point in the limit of zero emission technique.

D. Inflection point of a Langmuir probe

For completeness, the inflection point of a Langmuir probe method of measuring the plasma potential was compared in this paper to the emissive probe techniques. This method is not an emissive probe technique, but it is the other common probe technique for determining the plasma potential.[26] Probe theory suggests that an inflection point exists in the *I-V* trace of a Langmuir probe at the plasma potential in ideal conditions.[14] Ideal conditions, however, are rarely achieved and there are plasmas in which Langmuir probe techniques are difficult to use. If an electron beam is present in the plasma, an inflection point at the beam energy is created in the *I-V* trace which can be easily confused with the inflection point due to the plasma potential.[14,27] Additionally, the knee of an *I-V* trace is usually rounded due to contamination, potential fluctuations, and SEE effects (see Sec. III A).[14] The most persistent issue, however, is noise effects on the uncertainty of the measurement, which is discussed more thoroughly in Sec. V C. Only if the plasma is simple enough can the Langmuir probe technique be used to measure V_p.

IV. EXPERIMENTAL SETUP

A. Hall thruster

The various methods for measuring the plasma potential were tested in a 2 kW cylindrical Hall thruster (see Fig. 3). The Hall thruster itself is not of particular importance except as a plasma source. It was chosen as an ideal device for this experiment because conditions in such a plasma are far from ideal, with aspects including large potential and pressure gradients, relatively high T_e, flowing plasma, drifting electrons, magnetic field, beam electrons, high energy electrons from the cathode, and non-Maxwellian distributions.[19,21,28,29] Measurements were taken 0.5 cm axially away from the face of the thruster and between 0 and 0.2 cm radially inward from the outer edge. The plasmas examined in this region had a wide variety of temperatures and potentials, magnetic field, secondary electron emission effects, and ion drift.

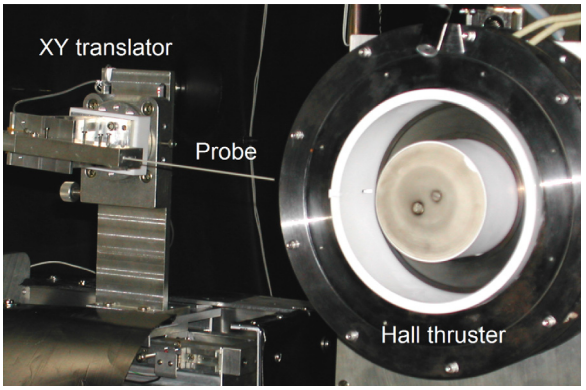

FIG. 3. (Color online) A photo of the Hall thruster used in the experiment as well as the probe and translational stage.

Additionally, simulations have predicted that the electron velocity distribution function (EVDF) in a Hall thruster is strongly non-Maxwellian and highly anisotropic.[30,31] Perpendicular to the walls, the EVDF has a depleted tail, while parallel to the walls (perpendicular to the face of the thruster), the EVDF has an enhanced tail. In order for an emissive probe technique to be robust, it must be able to make measurements with all of these non-ideal conditions affecting the probe.

The Hall thruster has an outer diameter of 12.3 cm, an inner diameter of 7.3 cm, and a channel depth of 4.6 cm. Two electromagnetic coils produced a magnetic field with a maximum strength of 100*G*, but only 50*G* at the measurement locations. The working gas, xenon, was flowed from the anode, which was biased between 250 and 450 V with respect to the cathode. This bias is known as the discharge voltage. The cathode was biased at −15 V with respect to ground. These discharge parameters created a plasma with $n_e \sim 10^9 - 10^{10}$ cm^{-3} and $T_e \sim 10-50$ eV (the plasma parameters varied across this range spatially within a single discharge). The large variation in electron temperature is due to the acceleration region and corresponding temperature gradient existing at different axial locations depending on the anode bias.[19] The characteristics of this device are explained in greater detail elsewhere.[13]

B. Emissive probe construction

A diagram of the emissive probe used is shown in Fig. 4. The alumina (Al_2O_3) tube was double bored to accommodate the two separate sets of wires leading to the probe. The probe was constructed by first inserting the probe filament made of 0.005 cm diameter thoriated tungsten so the wire stuck out the opposite end of the tube through both bores. The emissive probe wire was secured by inserting seven pieces of tungsten (not thoriated) wire of the same diameter into the bores but leaving the two tubes electrically connected only by the filament wire. The wires on the filament side of the tube were flush with the tube face but extended out the opposite end as a means of connecting the probe via interconnects to the wires leading to the circuitry. By inserting seven additional wires into each bore, the electrical contact and mechanical security were maintained. The total resistance across the whole probe construction was ∼2Ω. The boron nitride tube covered the 0.5 cm of alumina closest to the emitting wire which served to reduce secondary electron emission.

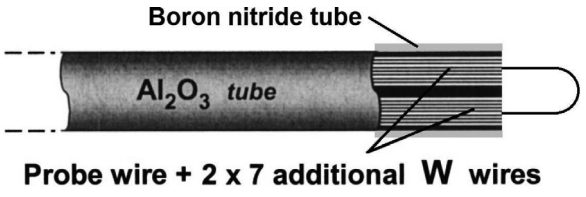

FIG. 4. A schematic diagram of the emissive probe design.

The probe was mounted on a two dimensional translator that could move the probe radial and axially. The alumina probe shaft was over 10 cm long, so the probe mount was far enough from the plasma as not to perturb it (see Fig. 3). As mentioned in Sec. IV A, the probe itself was moved very little and not at all while data were being taken.

C. Electronics

1. Floating point

As mentioned before, one reason for the floating point method's popularity is its ease of use, which can be seen in the electronics necessary to take measurements. A circuit diagram of the electronic system used to make measurements with the floating point method is shown in Fig. 5. The system consists of a power supply swept at a low frequency (∼0.1 Hz) with a triangular waveform which heats the emissive probe filament to emission. The power supply was a bipolar amplifier that was controlled by a function generator; the bipolar amplifier was used because almost 3 A of current was necessary to make the probe emit enough. The floating potential of the probe was measured using a high impedance operational amplifier to which was added one half of the heating voltage.[32] This adjustment was made to better estimate the potential at the point on the probe where the temperature was highest and emission was largest, which was assumed to be the middle of the filament.

2. I-V traces

The three other methods were performed by taking one or more *I-V* traces at various emission levels. The circuitry for all of these methods was the same, it was just in execution that they vary. Figure 6 shows the circuit diagram used

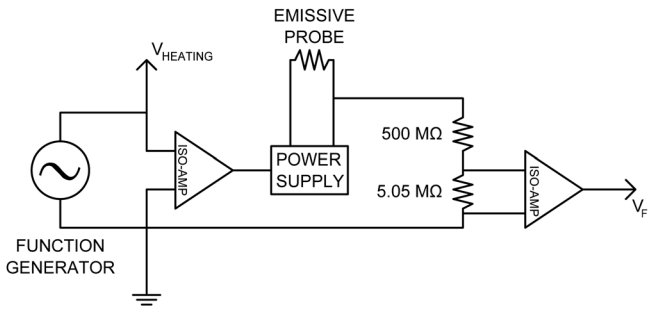

FIG. 5. The circuit diagram of the electronics used to measure the floating potential of an emissive probe at saturation.

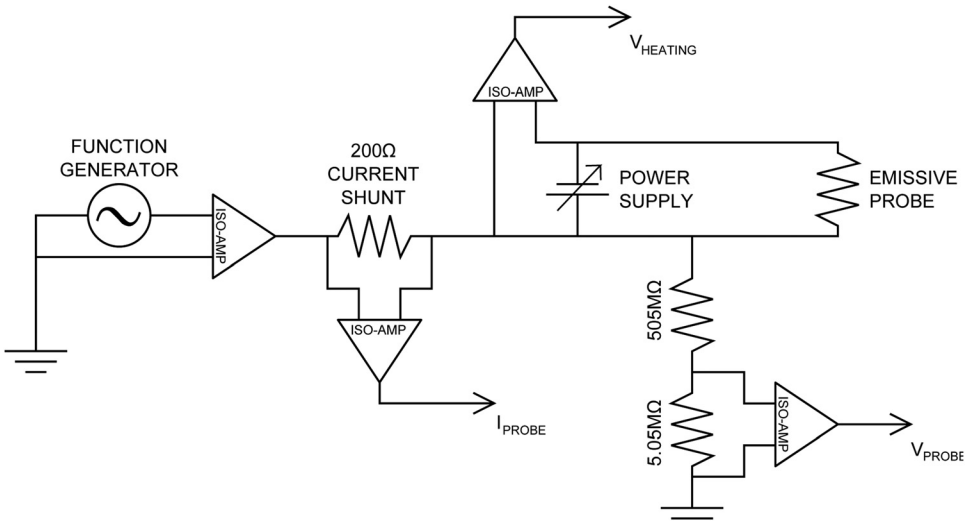

FIG. 6. The circuit diagram of the electronics used to take *I-V* traces.

to take emissive probe *I-V* traces. The bias on the probe was swept by a function generator with a sinusoidal waveform at 30 Hz amplified by a bipolar amplifier. A high sweep frequency was desired because when the probe was biased above the plasma potential, the collected electron current further heated the probe, leading to an inconsistent emission current over the *I-V* trace. However, if the frequency was too high, hysteresis would adversely affect the data. By setting the frequency to 30 Hz, the hysteresis and additional heating for high bias voltages were minimized, but both effects were present, requiring data to be taken only on the rising half cycle of the sweep. The probe was heated by a floating power supply that was manually controlled since the emission only needed to be changed between *I-V* traces, not during them. The probe current was determined by measuring the voltage across the 200Ω current shunt resistor. All measurement voltages were passed through isolation amplifiers before being recorded via a data acquisition (DAQ) card.

D. Data methods

1. Electron temperature

From probe measurements the electron temperature can be determined by fitting a line to the semilog graph of the characteristic cold *I-V* trace.[14] When the electron energy distribution function (EEDF) is non-Maxwellian, however, the determination of an effective electron temperature requires measurements of EEDF. In these experiments, the EEDF was not measured because that is a non-trivial task for magnetized plasmas and it was not the purpose of this work. The semilog *I-V* traces had two linear regions (see Fig. 7), indicative of a bi-Maxwellian EEDF. The linear region between 0 and 70 V is an approximately Maxwellian region and contains most of the plasma electrons. The region between −150 and 0 V is an enhanced high energy tail and describes only a small fraction of the plasma electrons. The temperature of the plasma used in the data analysis was the effective temperature combining the majority of colder electrons with the minority in the high energy tail. The temperature of the high energy tail ($T_{e,\mathrm{hot}}$) is the inverse of the slope of the line fitted to the −150 to 0 V region. The temperature of the colder electrons ($T_{e,\mathrm{cold}}$) is the inverse of the slope of the line fitted to the 0–70 V region after subtracting the contribution from the high energy tail. The fraction of electrons in the high energy tail (α) is equal to the current at the plasma potential due to the tail divided by the electron saturation current. Based on the kinetic definition of temperature,

$$T_e = \frac{1}{3} m_e \int_{-\infty}^{\infty} v^2 f(v) \mathrm{d}v, \tag{4}$$

an effective electron temperature can be derived by assuming that the EEDF is a bi-Maxwellian ($f(v) = \alpha f_h(v) + (1-\alpha) f_c(v)$, where $f_h(v)$ is the hot electron Maxwellian distribution function and $f_c(v)$ is the cold electron Maxwellian distribution function)

$$T_{e,\mathrm{eff}} = (1-\alpha) T_{e,\mathrm{cold}} + \alpha T_{e,\mathrm{hot}}. \tag{5}$$

This effective temperature is an approximation to account for the influence of the enhanced tail of the EEDF. For the example shown in Fig. 7, $T_{e,\mathrm{cold}} = 24.1$ eV, $T_{e,\mathrm{hot}} = 169$ eV, and $\alpha = 0.064$, resulting in $T_{e,\mathrm{eff}} = 33.3$ eV.

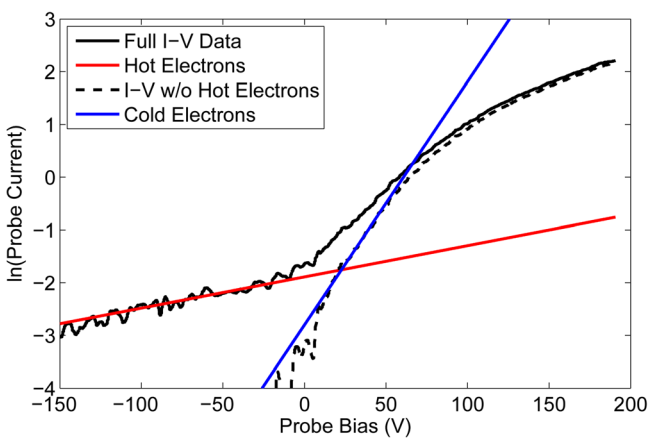

FIG. 7. (Color online) A typical semilog graph of an *I-V* curve with lines fit to the data to determine the temperature. The plasma potential is 109 V, $T_{e,\mathrm{cold}} = 24.1$ eV, $T_{e,\mathrm{hot}} = 169$ eV, $\alpha = 0.064$, and $T_{e,\mathrm{eff}} = 33.3$ eV. See text for comments on hot and cold electron temperatures.

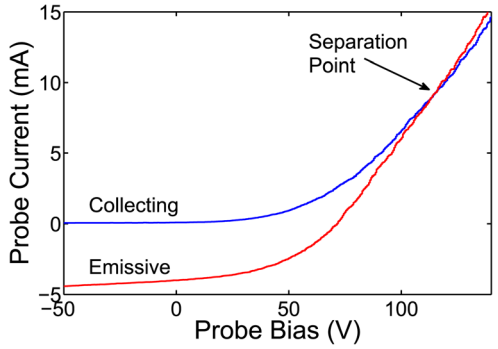

FIG. 8. (Color online) Typical data used to find the separation point. Note that where the separation point is indicated, the emitting and collecting curves cross.

The physical origin of the second electron group with $T_{e,\mathrm{hot}}$ exceeding 100 eV is not so clear. Particle in cell simulations of Hall thrusters have predicted the presence of SEE electron beams formed in the sheath.[33] According to these predictions, the SEE beam electrons could gain the maximum energy of ~100 eV and above depending on the electric and magnetic fields. However, it is not clear if the measured second slope is indeed a signature of these electrons. Without going into details of physics of the Hall thrusters, which is not the topic of this paper, we note that the current fraction of hot electrons is typically ~5% and therefore, the difference between T_e obtained from the slope for cold electrons and $T_{e,\mathrm{eff}}$ does not exceed 30%.

A different definition of effective temperature is commonly used when defining the Bohm velocity of ions in a two electron temperature plasma[34]

$$\frac{1}{T_{e,\mathrm{eff}}} = \frac{1-\alpha}{T_{e,\mathrm{cold}}} + \frac{\alpha}{T_{e,\mathrm{hot}}}. \tag{6}$$

This definition was not used because it is the EEDF that affects the floating potential of the emissive probe, not the velocity of ions at the sheath edge. The kinetic definition of effective temperature (Eq. (5)) is the more appropriate definition in this application. Using the definition given by Eq. (6) yields a slightly different effective electron temperature for the data in Fig. 7, $T_{e,\mathrm{eff}} = 25.5$ eV.

2. Separation point technique

Using the *I-V* trace electronics, two *I-V* traces were taken: one with the probe heated, but not to the point of emission, and one with the probe heated to emission (Fig. 8).[3,16] The emission must be large enough to distinguish the two curves near the plasma potential, so the authors chose the emission current to be approximately equal to the electron saturation current. As mentioned in Sec. III A, rather than separating at some point, the two curves cross. The reason for a crossing rather than a separation may be an increase in effective collecting probe radius as emission increases. The virtual cathode that forms around the probe would increase the effective collecting area, leading to a slightly larger collected electron current above the plasma potential, but whether or not the virtual cathode forms when the emitting surface is biased has not been established. There may be more complex factors at work, such as a non-monotonic relationship between heating current and electron saturation current, a result speculated to be caused by probe contamination.[35] This crossing point was taken to be the measure of the plasma potential which, in the case of the data in Fig. 8, is 114 ± 5 V.

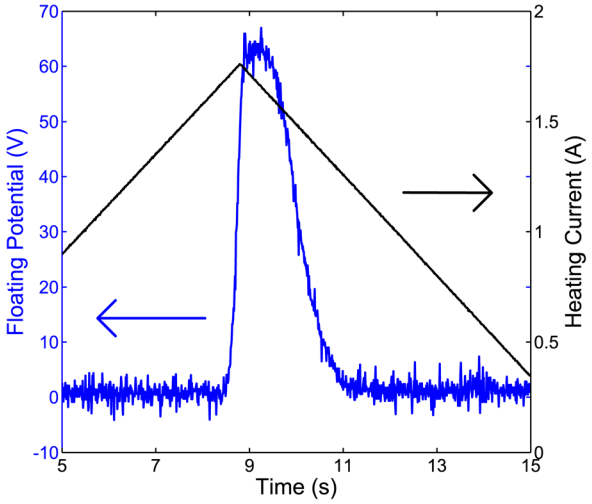

FIG. 9. (Color online) Typical data used to determine the floating point at saturation. The saturation occurs around a floating potential of 63 V, the voltage at which the floating potential does not increase beyond.

3. Floating point technique

Using the electronics described in Sec. IV C 1, a measure of the plasma potential can be made with the floating point method from data such as those shown in Fig. 9. The sawtooth shaped line is the heating current on the filament while the noisier line is the floating potential. The heating current line does not also indicate the temperature of the wire, as the wire can continue to increase in temperature even if the heating current is decreasing. Notice that the time corresponding to the peak of the heating current also is approximately the time at which the floating potential saturates. The plasma potential as measured by this technique is the potential at which the floating potential just begins to saturate, which is 63 ± 3 V in Fig. 9.[5]

4. Inflection point in the limit of zero emission technique

The inflection point in the limit of zero emission method requires that a number of *I-V* traces at small emission be taken, as is shown in Fig. 10. For these traces, the electron saturation current is difficult to determine but is certainly between 5 mA and 10 mA. The small bend at the maximum probe bias is a numerical artifact. Notice that it is not important that the temperature limited emissions be evenly spaced, but merely that there is a decent sample within the range. The inflection points can be determined by taking the derivative of the *I-V* traces and finding the maximum. These values are graphed versus the temperature limited emission, as is shown in Fig. 11. Linearly extrapolating to zero emission gives the inflection point in the limit of zero emission's measure of the plasma potential which is 102 ± 3 V.[6]

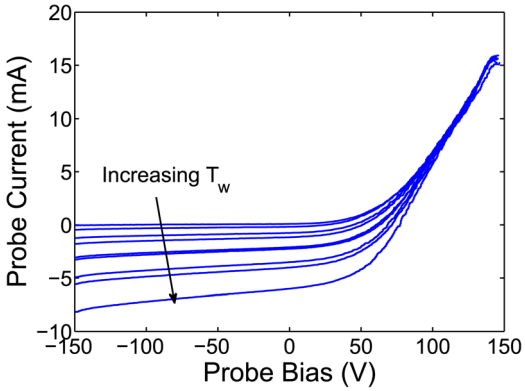

FIG. 10. (Color online) A typical set of *I-V* traces used for the inflection point in the limit of zero emission method.

5. Inflection point of a Langmuir probe technique

The inflection point of a Langmuir probe method was performed in exactly the same way as the inflection point in the limit of zero emission method except only one *I-V* trace was taken where there was no emission. Although the probe did not emit, it was still heated slightly which is not required for the technique, but it does keep the probe clean and helps to reduce noise from surface contamination. Figure 12 shows the derivative of a non-emissive *I-V* trace and identifies the inflection point which gives the measure of the plasma potential, which is 103 ± 20 V for the data in Fig. 12.

V. RESULTS

A. Analysis

Data were taken at a fixed location in plasmas with a wide variety of parameters ranging from $T_{e,\mathrm{eff}} = 13$ eV and $V_p = 63$ V when the discharge voltage was 250 V to $T_{e,\mathrm{eff}} = 48$ eV and $V_p = 188$ V where the discharge voltage was 450 V. In order for the comparison among the techniques to be meaningful, the measurements must be compared for the same plasma as described by the two discharge parameters: (a) anode bias and (b) anode current. Anode bias is set by a power supply and does not change except by raising or lowering the setting. The current, however, is determined

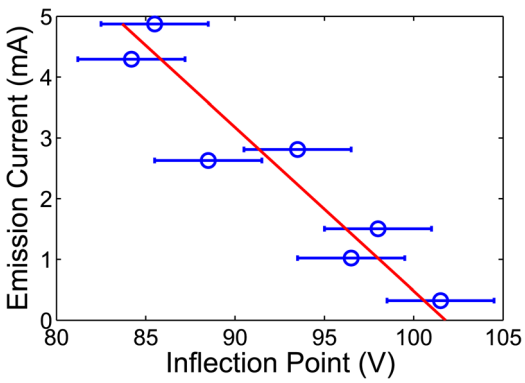

FIG. 11. (Color online) The inflection points and uncertainties as determined from the *I-V* traces in Fig. 10. The error bars are uncertainties in measuring the inflection point due to noise. The line is a linear fit to the data and extrapolated to zero emission.

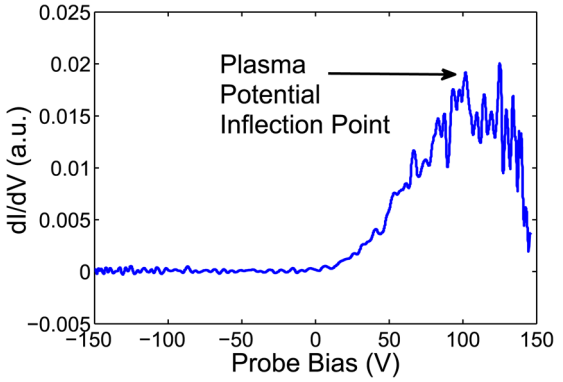

FIG. 12. (Color online) The derivative of a typical Langmuir probe *I-V* trace. The inflection point is difficult to identify because of the noise.

by the plasma itself and can change by a few percent over time (on the order of 10 min) even if controllable parameters have not been changed. Even a small change in discharge current can significantly affect the plasma potential at a fixed position.

B. Comparison among measurements of plasma potential

The difference between both inflection point methods and the floating point method is plotted against effective electron temperature (Eq. (5)) in Fig. 13. The dashed line indicating where the difference between the two measurements is $2T_{e,\mathrm{eff}}/e$ is included for reference. Notice that the inflection point in the limit of zero emission (V_{IP}) and the inflection point of a Langmuir probe (V_{LP}) agree quite closely with each other. Both measures of the plasma potential are consistently around $2T_{e,\mathrm{eff}}/e$ above the floating potential of a highly emissive probe. This is consistent with analytic and simulation predictions if the inflection point methods accurately measure the plasma potential. Were the Bohm velocity definition of effective electron temperature used (see Eq. (6)), the difference between the inflection point techniques and the floating point technique would be $\sim 2.5T_{e,\mathrm{eff}}/e$.

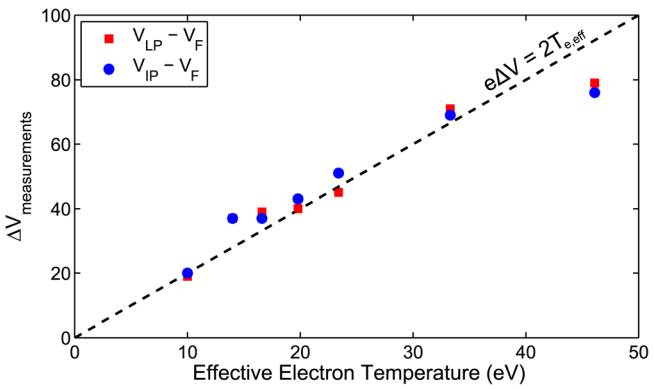

FIG. 13. (Color online) The differences between the inflection point in the limit of zero emission method and the floating point method ($V_{IP} - V_F$) and the inflection point of a Langmuir probe method and the floating point method ($V_{LP} - V_F$) versus electron temperature. The dashed line indicates where $e\Delta V_{measurements} = 2T_{e,\mathrm{eff}}$. This graph shows that a highly emitting surface floats $\sim 2T_{e,\mathrm{eff}}$ below the plasma potential as measured by the inflection point techniques.

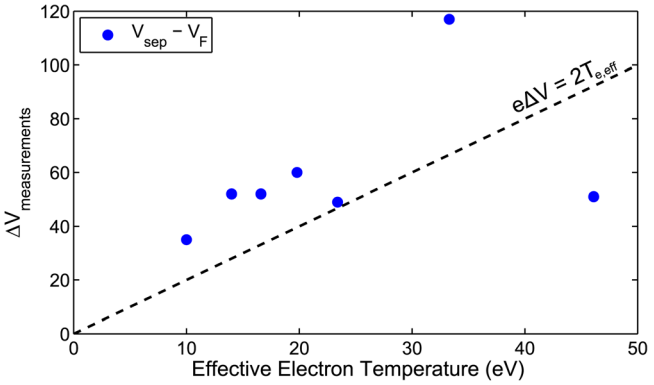

FIG. 14. (Color online) The difference between the separation point technique and the floating point technique versus temperature. Notice the large and varying differences between the two techniques.

Figure 14 shows the relationship between the separation point technique and the floating point technique. The difference between these two techniques varies wildly, between $T_{e,\mathrm{eff}}/e$ and $4T_{e,\mathrm{eff}}/e$. Because the floating point method is expected to have a consistent relationship to the plasma potential, it is reasonable to conclude that the separation point technique does not give a good measure of the plasma potential.

C. Uncertainty

An issue separate from that of what each method is actually measuring—the plasma potential or something else—is that of the uncertainty of the different techniques. The uncertainty arises from the construction of the method itself as well as the inherent noise of the plasma. Therefore, the uncertainties reported here are not universal, they only hold for the plasmas in which measurements were taken, but do still have qualitative significance. The authors suggest that the ordering in the uncertainty levels is the same for many plasmas.

The separation point method uncertainty arose from accurately identifying the potential at which the non-emitting and emitting *I-V* traces crossed. Typically, there was a range of voltages where the curves were almost coincident, the two lines crossing back and forth over each other, which was the principle cause of the $0.3T_{e,\mathrm{eff}}/e$ uncertainty. The uncertainty in the floating point method was due to the difficulty in identifying the saturation point of the floating potential. Both noise and the rounded knee contribute to the uncertainty which was typically $0.1T_{e,\mathrm{eff}}/e$. This number is the uncertainty in the measurement of the floating potential, not the uncertainty in the measurement of the plasma potential which has an additional $\sim T_{e,\mathrm{eff}}/e$ precision error. For the inflection point in the limit of zero emission, the uncertainty was dominated by that of fitting the line to the data. This uncertainty varied from plasma to plasma, but was typically around $0.1T_{e,\mathrm{eff}}/e$. The largest uncertainties were found in the Langmuir probe inflection point method. Because the measure of the plasma potential came directly from the derivative of data, any noise in the data was greatly amplified in the derivative. The uncertainty of this method was $0.5T_{e,\mathrm{eff}}/e$.

There is an additional source of uncertainty in this experiment that comes from not precisely knowing the potential on the emissive probe. The DC current used to heat the filament leads to a potential drop across the wire, typically of 3−4 V. Because of the strong temperature dependence on emission described by the Richardson-Dushman equation

$$J = A_G T_w^2 e^{\frac{-\phi_W}{T_w}} \tag{7}$$

where A_G is a material specific constant and ϕ_W is the work function, the greatest emission will be where the wire is hottest. The potential on the wire can be estimated as the potential at the hottest point since most electrons will be emitted that potential. It is difficult to know where the hottest point is on the filament, so it was approximated to be the middle of the wire.[36] To account for the potential drop, half of the heating voltage was added to the measured potential of the probe. The uncertainty from this measurement affects all measurements and was half of the heating voltage: ~2 V.

VI. CONCLUSIONS

Although the floating point technique is the most popular emissive probe method for measuring the plasma potential, these experiments have shown that it is not the most accurate. The inflection point methods' measurements are approximately $2T_{e,\mathrm{eff}}/e$ higher than the floating point method, which is consistent with theory if the inflection point methods accurately measure the plasma potential. Therefore, the inflection point methods do give an accurate measure of the plasma potential. In choosing between the inflection point in the limit of zero emission technique and the inflection point of a Langmuir probe technique, the former yielded a measurement with significantly less uncertainty than the latter because it is less influenced by noise. Additionally, it is known that emissive probes can determine the plasma potential in more systems than Langmuir probes can, such as in electron beams,[14,27] potential fluctuations,[1,22] and sheaths.[37] The authors suggest that the inflection point in the limit of zero emission technique be used as a standard for plasma potential measurements. After comparing another technique with it, one can determine the validity of the other technique for that specific application.

Although the inflection point methods provide the most accurate measurements of the plasma potential, the floating point method can still be useful. If no temperature gradients are present and the electron temperature is low $(eV_p/T_e \lesssim 1)$, the floating point method will still give a decent measure of the plasma potential.[12,13] Importantly, if there are no temperature gradients, the V_P measurements will have a constant offset, so calculations of the electric field will still be correct.

It is notable that even though the Hall thruster plasma is expected to be anisotropic and non-Maxwellian, the floating potential of an emitting surface is quite close to the predictions made with an isotropic, Maxwellian plasma. These results suggest that the tail of the distribution function does not play a significant role in determining the floating

potential of a strong electron emitting boundary. It has been shown that the high energy tail plays a significant role in determining the floating potential of a non-emitting boundary.[38] An emitting boundary, however, has a smaller potential barrier than a non-emitting boundary, so more low energy electrons can reach the boundary, reducing the effect of the tail. A more detailed investigation into the effects of the EEDF on the floating potential of an emitting surface must be done before any solid conclusions are drawn.

ACKNOWLEDGMENTS

Special thanks are due to Martin Griswold and Lee Ellison for all of their assistance. This work was supported by US Department of Energy grants No. DE-AC02-09CH11466, and No. DE-FG02-97ER54437, the DOE Office of Fusion Energy Science Contract DE-SC0001939, and the Fusion Energy Sciences Fellowship Program administered by Oak Ridge Institute for Science and Education under a contract between the U.S. Department of Energy and the Oak Ridge Associated Universities.

[1]E. Y. Wang, N. Hershkowitz, T. Intrator, and C. Forest, Rev. Sci. Instrum. **57**, 2425 (1986).
[2]R. Schrittwieser, J. Adamek, P. Balan, M. Hron, C. Ionita, K. Jakubka, L. Kryska, E. Martines, J. Stockel, M. Tichy, and G. Van Oost, Plasma Phys. Controlled Fusion **44**, 567 (2002).
[3]F. F. Chen, in *Plasma Diagnostic Techniques*, edited by R. H. Huddlestone and S. L. Leonard (Academic, New York, 1965) Chap. IV, p. 184.
[4]C. R. Hoffmann and D. J. Lees, Plasma Phys. **13**, 689 (1971).
[5]R. F. Kemp and J. M. Sellen, Rev. Sci. Instrum. **37**, 455 (1966).
[6]J. R. Smith, N. Hershkowitz, and P. Coakley, Rev. Sci. Instrum. **50**, 210 (1979).
[7]G. D. Hobbs and J. A. Wesson, Plasma Phys. **9**, 85 (1967).
[8]L. A. Schwager, Phys. Fluids B Plasma Phys. **5**, 631 (1993).
[9]V. A. Rozhansky and L. D. Tsendin, *Transport Phenomena in Partially Ionized Plasma* (Taylor and Francis, London, New York, 2001) pp. xiv, 469 p.
[10]K. U. Riemann, Phys. Plasmas **13**, 063508 (2006).
[11]T. Intrator, M. H. Cho, E. Y. Wang, N. Hershkowitz, D. Diebold, and J. Dekock, J. Appl. Phys. **64**, 2927 (1988).
[12]L. Dorf, Y. Raitses, and N. J. Fisch, Rev. Sci. Instrum. **75**, 1255 (2004).
[13]Y. Raitses, D. Staack, A. Smirnov, and N. J. Fisch, Phys. Plasmas **12**, 073507 (2005).
[14]N. Hershkowitz, in *Plasma Diagnostics*, edited by O. Auciello and D. L. Flamm (Academic, New York, 1989), Vol. 1, pp. 113–183.
[15]M. J. M. Parrot, L. R. O. Storey, L. W. Parker, and J. G. Laframboise, Phys. Fluids **25**, 2388 (1982).
[16]I. Langmuir, J. Franklin Inst. **196**, 751 (1923).
[17]K. Inai, K. Ohya, G. Kawamura, and Y. Tomita, Contrib. Plasma Phys. **50**, 458 (2010).
[18]H. Fujita and S. Yagura, Jpn. J. Appl. Phys., Part 1 **22**, 148 (1983).
[19]D. Staack, Y. Raitses, and N. J. Fisch, Appl. Phys. Lett. **84**, 3028 (2004a).
[20]J. W. Bradley, S. Thompson, and Y. A. Gonzalvo, Plasma Sources Sci. Technol. **10**, 490 (2001).
[21]J. M. Haas and A. D. Gallimore, Phys. Plasmas **8**, 652 (2001).
[22]R. Schrittwieser, C. Ionita, P. Balan, C. Silva, H. Figueiredo, C. A. F. Varandas, J. J. Rasmussen, and V. Naulin, Plasma Phys. Controlled Fusion **50**, 8 (2008).
[23]N. Mahdizadeh, F. Greiner, M. Ramisch, U. Stroth, W. Guttenfelder, C. Lechte, and K. Rahbarnia, Plasma Phys. Controlled Fusion **47**, 569 (2005).
[24]X. Wang and N. Hershkowitz, Rev. Sci. Instrum. **77** (2006).
[25]M. Y. Ye and S. Takamura, Phys. Plasmas **7**, 3457 (2000).
[26]V. A. Godyak, R. B. Piejak, and B. M. Alexandrovich, Plasma Sources Sci. Technol. **1**, 36 (1992).
[27]T. Gyergyek, J. Kovacic, and M. Cercek, Contrib. Plasma Phys. **50**, 121 (2010).
[28]D. Staack, Y. Raitses, and N. J. Fisch, Rev. Sci. Instrum. **75**, 393 (2004).
[29]N. B. Meezan, W. A. Hargus, and M. A. Cappelli, Phys. Rev. E **63** (2001).
[30]I. D. Kaganovich, Y. Raitses, D. Sydorenko, and A. Smolyakov, Phys. Plasmas **14**, 057104 (2007).
[31]D. Sydorenko, A. Smolyakov, I. Kaganovich, and Y. Raitses, IEEE Trans. Plasma Sci. **34**, 815 (2006).
[32]S. Iizuka, P. Michelsen, J. J. Rasmussen, R. Schrittwieser, R. Hatakeyama, K. Saeki, and N. Sato, J. Phys. E **14**, 1291 (1981).
[33]D. Sydorenko, A. Smolyakov, I. Kaganovich, and Y. Raitses, Phys. Plasmas **13**, 014501 (2006).
[34]R. W. Boswell, A. J. Lichtenberg, and D. Vender, IEEE Trans. Plasma Sci. **20**, 62 (1992).
[35]A. Marek, M. Jilek, I. Pickova, P. Kudrna, M. Tichy, R. Schrittwieser, and C. Ionita, Contrib. Plasma Phys. **48**, 491 (2008).
[36]W. E. Yao, T. Intrator, and N. Hershkowitz, Rev. Sci. Instrum. **56**, 519 (1985).
[37]H. Yamada and D. L. Murphree, Phys. Fluids **14**, 1120 (1971).
[38]V. I. Demidov, C. A. DeJoseph, and A. A. Kudryavtsev, Phys. Rev. Lett. **95**, 4 (2005).